



Article

Constitutive Expression of *Aechmea fasciata* SPL14 (*AfSPL14*) Accelerates Flowering and Changes the Plant Architecture in *Arabidopsis*

Ming Lei ^{1,2,3,4}, Zhi-ying Li ^{1,2,3,4}, Jia-bin Wang ^{1,2,3,4}, Yun-liu Fu ^{1,2,3,4}, Meng-fei Ao ^{1,2,3,4} and Li Xu ^{1,2,3,4,*}

¹ Institute of Tropical Crops Genetic Resources, Chinese Academy of Tropical Agricultural Sciences, Danzhou 571737, China; leiming_catas@126.com (M.L.); xllizhiying@vip.163.com (Z.-y.L.); jiabinwangfuhu@sina.com (J.-b.W.); fyljj_2007@126.com (Y.-l.F.); 17889981612@163.com (M.-f.A.)

² Key Laboratory of Crop Gene Resources and Germplasm Enhancement in Southern China, Danzhou 571737, China

³ Key Laboratory of Tropical Crops Germplasm Resources Genetic Improvement and Innovation, Danzhou 571737, China

⁴ Mid Tropical Crop Gene Bank of National Crop Resources, Danzhou 571737, China

* Correspondence: xllzy@263.net; Tel.: +86-898-2330-0284

Received: 21 June 2018; Accepted: 14 July 2018; Published: 18 July 2018



Abstract: Variations in flowering time and plant architecture have a crucial impact on crop biomass and yield, as well as the aesthetic value of ornamental plants. *Aechmea fasciata*, a member of the Bromeliaceae family, is a bromeliad variety that is commonly cultivated worldwide. Here, we report the characterization of *AfSPL14*, a squamosa promoter binding protein-like gene in *A. fasciata*. *AfSPL14* was predominantly expressed in the young vegetative organs of adult plants. The expression of *AfSPL14* could be upregulated within 1 h by exogenous ethephon treatment. The constitutive expression of *AfSPL14* in *Arabidopsis thaliana* caused early flowering and variations in plant architecture, including smaller rosette leaves and thicker and increased numbers of main inflorescences. Our findings suggest that *AfSPL14* may help facilitate the molecular breeding of *A. fasciata*, other ornamental and edible bromeliads (e.g., pineapple), and even cereal crops.

Keywords: *Aechmea fasciata*; squamosa promoter binding protein-like; flowering time; plant architecture; bromeliad

1. Introduction

The squamosa promoter binding protein (SBP)-like (SPL) proteins are plant-specific transcription factors (TFs) that play essential roles in the regulation networks of plant growth and development [1]. The genes encoding SPL proteins were first identified in snapdragon (*Antirrhinum majus*), and were then found in almost all other green plants [2–5]. All SPL proteins contain a highly conserved DNA-binding domain termed the SBP domain, which consists of approximately 76 amino acid residues and features two zinc-binding sites and a bipartite nuclear localization signal (NLS) [6]. Many studies of various species have revealed the diverse functions of SPLs, which are involved in a broad range of important biological processes including the leaf development [7–10], embryonic development [11], fertility controlling [12,13], copper homeostasis [14,15], as well as the biosynthesis of phenylpropanoids and sesquiterpene. In addition to affecting these developmental aspects, several SPL factors which can be regulated by miR156, an evolutionary highly conserved microRNA (miRNA), also play crucial roles in the control of flowering time. The overexpression of *AtSPL3*, *AtSPL4*, *AtSPL5*, *AtSPL9*, *AtSPL15*, and *OsSPL16* can significantly promote flowering [3,9,16–19]. *AtSPL9*, together with *AtSPL3* and

the AtSPL2/10/11 group promote the floral meristem identity by directly regulating the same or different target genes [9,19]. Interestingly, compared with the positive regulation of accelerated flowering by the SPLs described above, AtSPL14 appears to be a negative regulator of vegetative-phase changes and floral transitions [20]. Another function of miR156-regulated SPL factors is in plant architecture formation and yield. *Teosinte Glume Architecture (TGA1)*, an SPL gene, is responsible for the liberation of the kernel during domestication and evolution in *Z. mays* [21]. In *Triticum aestivum*, TaSPL3/17 play important roles in reducing the number of tillers and the outgrowth rate of axillary buds [22]. Two SPL homologs, TaSPL20 and TaSPL21, together reduce plant height and increase the thousand-grain weight [23]. In switchgrass (*Panicum virgatum*), miR156-regulated SPL4 suppresses the formation of both aerial and basal buds and controls the shoot architecture [24]. In *O. sativa*, higher expression of *OsSPL14* can reduce the tiller number, increase the lodging resistance, promote panicle branching and enhance grain yields [25,26]. The multifaceted functions of SPLs demonstrate complex and interesting regulation networks underlying plant lifestyles.

Bromeliaceae is one of the most morphologically diverse families and is widely distributed in tropical and subtropical areas [27]. Although certain cultivated species of bromeliads are appreciated for their edible fruits (e.g., pineapple: *Ananas comosus*) or medicinal properties (e.g., *Bromelia antiacantha*), the vast majority are appreciated for their ornamental value [28]. However, the unsynchronized natural flowering time of cultivated bromeliads always results in increased cultivation and harvesting costs and decreased economic value of fruits and ornamental flowers [29]. To date, several efforts were made to uncover the mechanism of flowering of bromeliads induced by age, photoperiod, autonomous and exogenous ethylene, or ethephon [29–33], but the precise molecular mechanism remained unknown.

Here, we characterized the SPL gene *AfSPL14*, from *Aechmea fasciata*, a popular ornamental flowering bromeliad. Phylogenetic analyses showed that *AfSPL14* is closely related to *OsSPL17*, *OsSPL14*, *AtSPL9*, and *AtSPL15*. Furthermore, the expression of *AfSPL14* transcripts responded to plant age and exogenous ethephon treatment. The constitutive expression of *AfSPL14* in *Arabidopsis* promotes branching and accelerates flowering under long-day (LD) conditions. These results suggested that *AfSPL14*, a TF of the SPL family, might be involved in the process of flowering and in plant architecture variations of *A. fasciata*.

2. Results

2.1. Isolation and Sequence Analysis of *AfSPL14* in *A. fasciata*

The SPL cDNA was isolated using the rapid amplification of cDNA ends (RACE) technique, and then named *AfSPL14*. The cDNA of *AfSPL14* was 1504-bp long and presented a 123-bp 5' untranslated region (UTR), a 331-bp 3' UTR, and a 1050-bp open reading frame (ORF), which was predicted to encode a 349-amino acid protein with a molecular weight (MW) and an isoelectric point (pI) of 37.53 kDa and 9.08, respectively.

To investigate the evolutionary relationships between the *AfSPL14* and SPL proteins of other species, a phylogenetic tree was constructed using the neighbor-joining method with 1000 bootstrap replicates with 13 SBPs of *Physcomitrella patens*, 16 SPLs of *Arabidopsis*, and 19 SPLs of *O. sativa* (Table S1). Because the alignment of the full-length protein sequences showed no consensus sequences except for SBP domains (data not shown), only the highly-conserved SBP domains were used for the phylogenetic analysis. The unrooted phylogenetic tree classified all SBP domains into seven groups (I–VII), and *AfSPL14* was clustered into group III, with *AtSPL9*, *AtSPL15*, *OsSPL7*, *OsSPL14*, and *OsSPL17*; however, this group did not contain SBP domains of *P. patens* (Figure 1), which was similar to the results obtained by others [34]. The fact that *AfSPL14* has been classified with three SPL genes in *O. sativa* and two in *Arabidopsis* suggests that the SBP domains of these six SPLs might have undergone species-specific evolutionary processes after speciation.

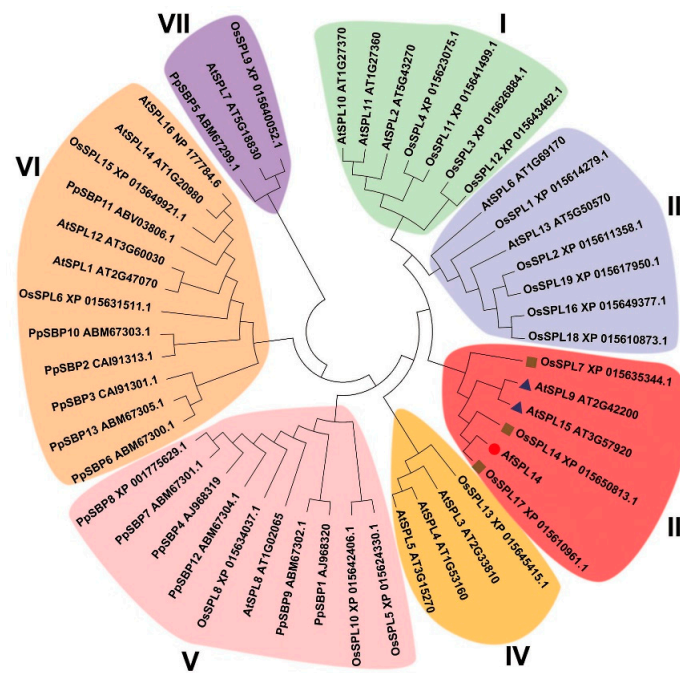


Figure 1. Phylogenetic analysis of AfSPL14 and SPLs of *Arabidopsis*, *O. sativa* and *P. patens* based on the conserved SBP domains. The unrooted tree was created using the neighbor-joining method with 1000 bootstrap replicates with 13 SBPs of *P. patens*, 16 SPLs of *Arabidopsis*, and 19 SPLs of *O. sativa*. The sequences of all these SBP domains are listed in Table S1.

The multiple sequence alignment of the AfSPL14 protein with SPL homologs of other species indicated that the SBP domain was highly conserved among the species (Figure 2a). All SBP domains could be divided into four motifs, which were zinc finger-like structure 1 (Zn1), Zn2, joint peptide (Jp) of Zn1 and Zn2, and NLS. The first zinc finger was C4H, and the second zinc finger-like structure was C2HC. The Jp plays a crucial role in modifying the protein-DNA interaction process [6], and was also highly conserved in all aligned sequences (Figure 2a). In addition, the bipartite NLS motif, which partially overlapped Zn2, was highly conserved (Figure 2a,b).

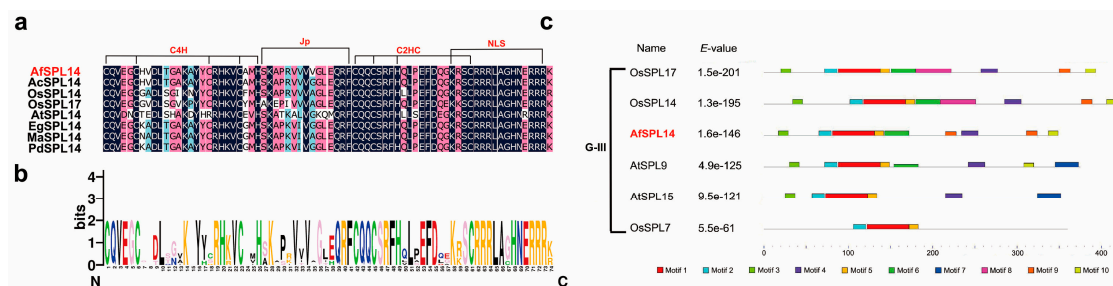


Figure 2. Sequence alignment and logo view of variable SBP domains, and putative motifs of variable SPLs in group III. (a) Multiple alignment of the SBP domains using DNAMAN software. The four conserved motifs, which include two zinc finger-like structures (C4H, C2HC), Jp and NLS, are indicated; (b) Sequence logo view of the consensus SBP domains. The overall height of the stack and the height of each letter represent the sequence conservation at that position and the relative frequency of the corresponding amino acid at that position, respectively; (c) putative motifs of variable SPLs in group III identified by MEME software online (<http://meme-suite.org/tools/meme>). The color boxes represent different putative motifs for which the sequences are listed in Table S2 online. G-III indicates group III from Figure 1.

To further examine conserved sequences other than the SBP domain, the online Multiple EM for Motif Elicitation (MEME) tool was used to identify putative motifs in the SPL proteins in group III [35]. As shown in Figure 2c, all members of group III contained motifs 1, 2, and 5, and these motifs had similar distributions. Actually, motif 2 belongs to C4H, and motif 5 belongs to NLS; motif 1 contains Jp, C2HC, and partials of C4H and NLS (Figure 2c, Table S2). Compared with OsSPL14 and OsSPL17, which contained all motifs except motif 7, AfSPL14 had a similar motif distribution but lacked motifs 7 and 8 (Figure 2c). These results suggested that AfSPL14 might have conserved functions with OsSPL14 and OsSPL17.

Exon-intron organization of all members of group III genes were generated based on genome sequences and the corresponding CDSs (Figure 3). As shown in Figure 3, each member of these genes had two introns and three exons; thus, they shared a similar exon-intron composition. All members of rice and *Arabidopsis* in group III were targets of miR156 [9,36], and a putative miR156 target site was also observed in AfSPL14 (Figure 3). The consistency of the motif investigation, exon-intron organization, and phylogenetic analysis indicates putative similarities in functional regions and sites among the genes in group III.

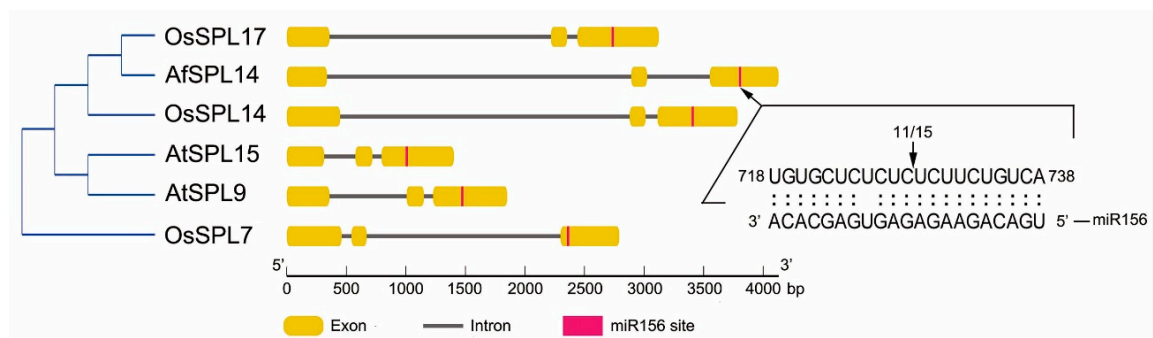


Figure 3. Exon-intron structures of SPL genes in group III from Figure 2 and AfmiR156 cleavage site in AfSPL14 determined by 5' RLM-RACE. For the determination of the AfmiR156 cleavage site in AfSPL14, 15 clones were selected randomly for sequencing, and 11 of them were cleaved in the position indicated by the arrow towards the base interval of AfSPL14 RNA sequence.

2.2. AfSPL14 Was a Target of miR156 of *A. fasciata* (AfmiR156)

As all members of rice and *Arabidopsis* in group III were targets of miR156, there was also a putative miR156 target site in AfSPL14 (Figure 3). To test whether the mRNA of AfSPL14 was indeed targeted for degradation and was cleaved at the predicted position by AfmiR156, 5' RNA ligase mediated rapid amplification of cDNA ends (RLM-RACE) was carried out to map the 5' terminus of the cleavage fragment. DNA sequencing results of the amplified product demonstrated that AfSPL14 could be indeed cleaved by AfmiR156 (Figure 3).

2.3. Transcript Profiling of AfSPL14 in *A. fasciata*

To gain insights into the role of AfSPL14 in *A. fasciata*, we determined the gene's expression profiles in various organs at different developmental stages via reverse transcription followed by quantitative real-time PCR (RT-qPCR). The transcripts of AfSPL14 could be detected in almost all tested tissues except the roots of the adult plant prior to flower bud differentiation (Figure 4a). AfSPL14 mRNA was more abundant in the central leaves and stems regardless of the developmental stage (Figure 4a,b). The accumulation of AfSPL14 transcripts in the central leaves and stems showed significant changes during development, with the highest level observed in adult plants prior to flower bud differentiation, a relatively lower level observed in juvenile plants, and the lowest level observed in 39-day-after-flowering (DAF) adult plants (Figure 4a,b), suggesting that AfSPL14 might be involved in phase transitions.

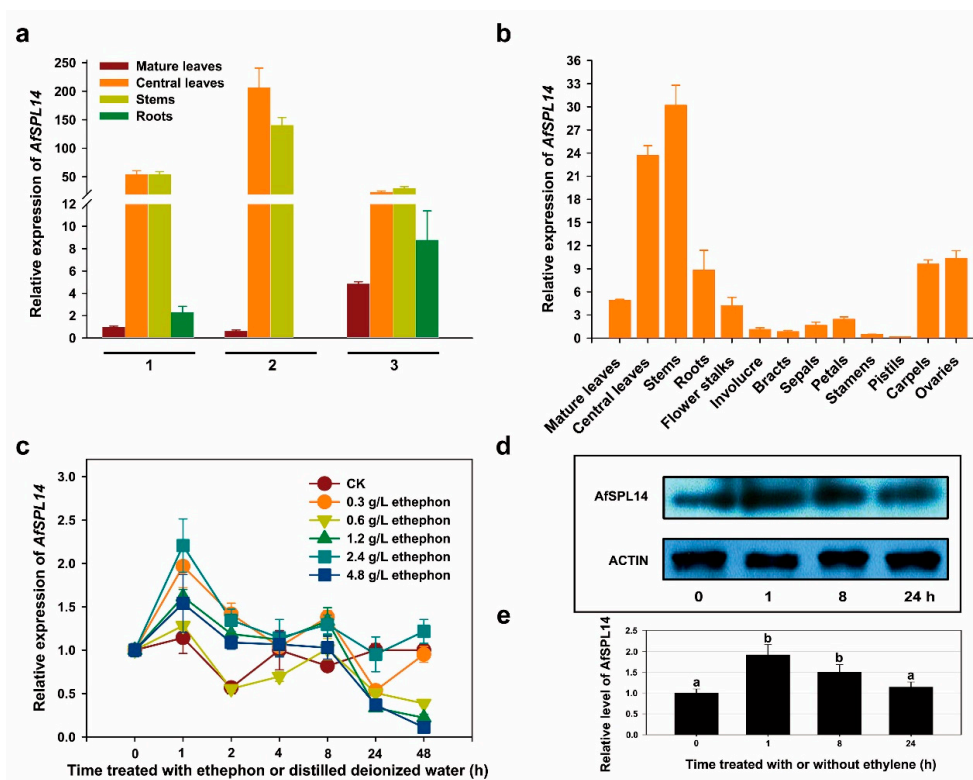


Figure 4. Expression of *AfSPL14* transcripts in various tissues of *A. fasciata* and immunoblot analysis of *AfSPL14* in central leaves treated with or without ethephon. (a) Expression level of *AfSPL14* transcripts in various tissues of juvenile and adult plants. (1) juvenile plants; (2) adult plants prior to flower bud differentiation; (3) 39-DAF flowering adult plants. Samples were collected at 10:00 am. (b) Expression level of *AfSPL14* transcripts in the vegetative and reproductive organs of 39-DAF flowering adult plants. Samples were collected at 10:00 am. (c) Expression level of *AfSPL14* transcripts in the central leaves of *A. fasciata* in response to exogenous ethephon treatment at different concentrations for different time. In the panels, 0, 1, 2, 4, and 8 h represents the samples collected at 10:00, 11:00, 12:00, 14:00, and 18:00, respectively; 24 h and 48 h represent the treated samples collected at 10:00 am at the next day and the next two days, respectively. For CK, 10 mL of distilled deionized H₂O was poured into the cylinder shapes of *A. fasciata*. 0 h represents the samples treated without ethephon or distilled deionized H₂O. (d) Immunoblot analysis of the *AfSPL14* protein level in the central leaves of *A. fasciata* treated with 10 mL of 0.6 g·L⁻¹ exogenous ethephon for 1, 8, and 24 h, or without ethephon (0 h). The total proteins were separated using SDS-PAGE, and the transferred proteins were then probed with a rabbit polyclonal *AfSPL14* antibody or a rabbit polyclonal Actin antibody, respectively. (e) Relative level of *AfSPL14* protein in the central leaves of *A. fasciata* treated with 10 mL of 0.6 g·L⁻¹ exogenous ethephon for 1, 8 and 24 h, or without ethephon (0 h). Three independent experiments were performed, the values are shown as the means and error bars indicate the standard deviation ($n = 3$). ANOVA was conducted, and means were separated by DNMRT.

2.4. Response to Exogenous Ethephon Treatment

To induce bromeliad flowering, ethylene or ethephon is widely used [29]. In fact, flowering induction by ethylene or ethephon is age-dependent. Plants of *A. comosus* which were somewhat less than about 1.0 kg fresh weight in subtropical regions respond only minimally to ethylene or ethephon [29]. Similar to ‘Smooth Cayenne’ and other variations of *A. comosus*, adult plants (but not juveniles) of *A. fasciata* could be induced by ethephon. Our previous investigation also showed that above 96% of 12-month-old adult plants could be induced to flower by 10 mL of exogenous ethephon treatment at 0.6 g·L⁻¹ within two weeks, but that none of 6-month-old juvenile plants flowered under the same condition [37]. Here, we investigated the possible response of *AfSPL14* in

adult plants of *A. fasciata* to exogenous ethephon treatment at different concentrations. As shown in Figure 4c, the expression of *AfSPL14* transcripts in the central leaves of adult plants prior to flower bud differentiation increased transiently after treatment for 1 h. Interestingly, a rapid decrease of the expression level of *AfSPL14* transcripts was observed after treatment for 2 h, almost reaching lower levels than in control plants after 24 h (Figure 4c), suggesting the remarkable effect of ethylene on the expression of *AfSPL14*.

To investigate the effect of ethylene on the level of AfSPL14 protein, we extracted the total proteins from the central leaves of *A. fasciata* treated with or without 10 mL of 0.6 g·L⁻¹ ethephon. An immunoblot analysis was performed using a specific antibody against the AfSPL14 protein (Figure 4d). The level of AfSPL14 after treatment for 1 h was ~200% higher than the level in the untreated central leaves (Figure 4d,e). Consistent with the changes in the relative expression of *AfSPL14* mRNA, the level of AfSPL14 also gradually decreased after continuous treatment for 8 and 24 h (Figure 4d,e).

2.5. *AfSPL14* Does Not Exhibit Transactivation Activity in Yeast

To test whether AfSPL14 is a transcriptional activator, the ORF (1-349 amino acids), the N terminus containing the SBP domain (1-141 amino acids) (AfSPL14N), and the C terminus (142-349 amino acids) (AfSPL14C) of AfSPL14 were fused with the GAL4 binding domain carried by the pGBKT7 (pBD) vector, respectively. The expression vectors pBD-AfSPL14, pBD-AfSPL14N, and pBD-AfSPL14C were then transformed into the yeast strain Y2HGOLD carrying the dual reporter genes *AUR1-C* and *MEL1*, respectively. As shown in Figure 5, similar to the negative control pBD, but not the positive control pGAL4, all the yeast cells carrying the three tested vectors could not grow on a medium containing SD/-Trp/+AbA/+X- α -Gal, indicating that AfSPL14 could not activate the transcription of the dual reporter genes in yeast.

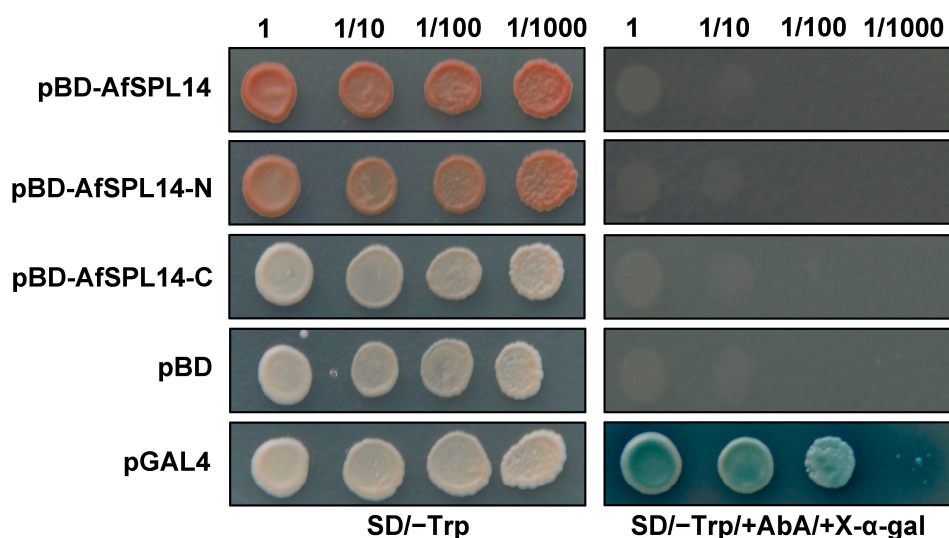


Figure 5. Transactivation activity assay of AfSPL14 in yeast cells. The pGBKT7 (pBD) vectors were fused with the full-length of AfSPL14 (pBD-AfSPL14), the N terminus of AfSPL14 (pBD-AfSPL14-N) and the C terminus of AfSPL14 (pBD-AfSPL14-C), respectively. Each kind of these constructs was then transformed into Y2HGOLD cells which contained the reporter genes *AUR1-C* and *MEL1*. pBD and pGAL4 plasmids were transformed into Y2HGOLD cells and used as negative and positive controls, respectively. Yeast clones containing the right constructs grew on SD/-Trp medium at dilutions of 1, 1/10, 1/100, and 1/1000 for three to five days, and were then transferred onto SD/-Trp/+AbA/+X- α -Gal medium for continuous growth for three further days to test their transactivation activities. SD: synthetic dropout; AbA: Aureobasidin A; SD/-Trp: SD medium without Trp; SD/-Trp/+AbA/+X- α -gal: SD medium without Trp, but with 40 mg/L X- α -gal and 200 μ g/L AbA.

2.6. Constitutive Expression of *AfSPL14* in *Arabidopsis*

To assess the function of *AfSPL14* in flowering, we induced the ectopic expression of *AfSPL14* with the 35S CaMV promoter (*Pro35S::AfSPL14*) in *Arabidopsis* ecotype Columbia (Col-0) (WT) (Figure S1). Under LD conditions, the flowering time of *Pro35S::AfSPL14* transgenic plants was significantly earlier ($p = 6.26 \times 10^{-8}$) than that of the WT and the WT transformed with the empty vector (Vector) (Figure 6a–c). Although the difference of the number of rosette leaves was minor between the *Pro35S::AfSPL14* transgenic plants and WT, the statistical analysis indicated that the number was significantly lower ($p = 4.69 \times 10^{-5}$) in the *Pro35S::AfSPL14* transgenic plants (Figure 6c). The *Pro35S::AfSPL14* transgenic lines were also smaller than the WT (Figure 6a–c). In addition, the *Pro35S::AfSPL14* transgenic plants showed morphological changes in the reproductive phase. A comparison between the WT and Vector, which only has one main inflorescence per plant, showed that a majority of the transformants of *Pro35S::AfSPL14* developed two main inflorescences (Figure 6b,d). Interestingly, a second inflorescence could be developed from the base of the main inflorescence, and it could also develop from the node of the main inflorescence or even be divided randomly from the non-node position of the main inflorescence (Figure 6b,d). Another change in the reproductive phase was the thickening of the main inflorescence in the *Pro35S::AfSPL14* transgenic plants compared with that of the WT (Figure 6e,f).

To further confirm whether the expression of *AfSPL14* in the *Pro35S::AfSPL14* transgenic plants altered the expression of downstream flowering genes, RT-qPCR analysis was performed with the *Arabidopsis* shoot apices grown under LD conditions as materials. The *Arabidopsis* shoot apices were harvested from the central parts of *Arabidopsis* seedlings, and contain the youngest rosette leaves. As expected, compared to WT, the expression level of the genes *SUPPRESSOR OF OVEREXPRESSION OF CONSTANS 1* (*SOC1*), *FRUITFULL* (*FUL*) and *APETALA1* (*AP1*), which encode floral inductive factors, was substantially upregulated at the shoot apex of *Pro35S::AfSPL14* transgenic plants (Figure 7a,b,e). However, the expression level of another gene encoding plant-specific transcription factor *LEAFY* (*LFY*), which is also a positive regulator inducing flowering at the shoot apex, showed no clear difference between WT and *Pro35S::AfSPL14* transgenic plants (Figure 7c). The expression level of *Flowering Locus T* (*FT*), an integrator of flowering pathways and defined as a florigen, was also considerably upregulated at the shoot apex of *Pro35S::AfSPL14* transgenic plants (Figure 7d). In addition, the expression of floral organ identity genes, such as *AtAP2* and *AtAP3*, was also upregulated (Figure 7f,g).

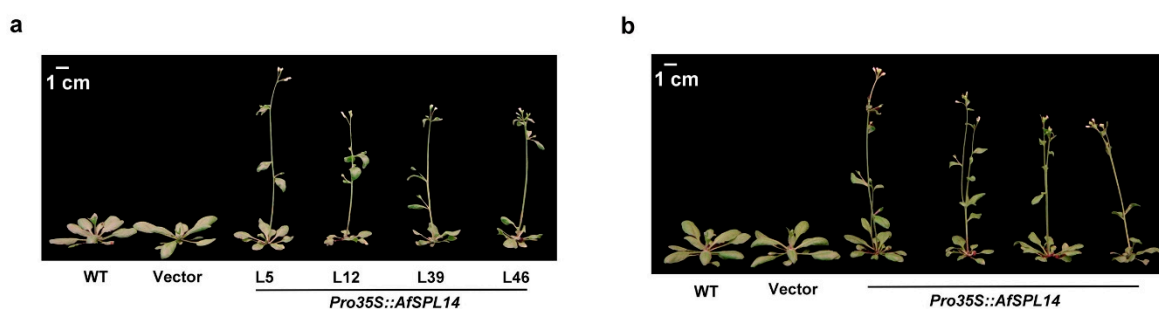


Figure 6. Cont.

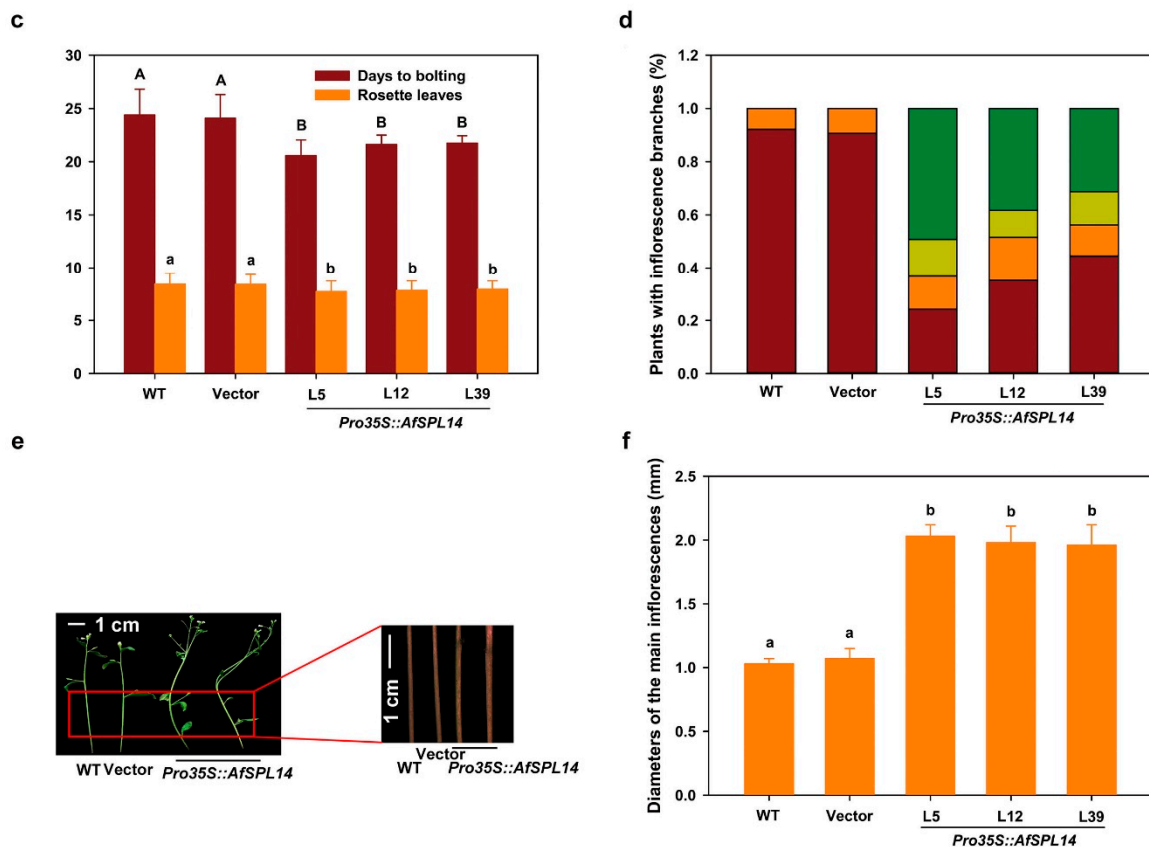


Figure 6. Phenotype analysis of *Pro35S::AfSPL14* transgenic plants. (a) Flowering *Pro35S::AfSPL14* transgenic plants shown next to WT and WT transformed with the empty vector (Vector) under LD conditions. L5, L12, L39, and L46 indicate the different lines. (b) Flowering *Pro35S::AfSPL14* transgenic plants that had two main inflorescences under LD conditions. (c) Days and number of rosette leaves to bolting of the WT, Vector and *Pro35S::AfSPL14* transgenic plants grown under LD conditions. Values are the means \pm standard deviation. Seventy-nine plants were scored for each line. Difference letters indicate statistical differences. (d) Percentages of plants which have two main inflorescences grown under LD conditions. The number of plants with the second main stem developed from the base (orange), the node (ginger), and the non-node (dark green) position of the main inflorescences and plants with only one inflorescence (dark red) was calculated. One hundred and twenty-eight 38-day-old, long-day-grown plants and ninety-six 55-day-old, short-day-grown plants were counted for each line. (e) Bending and thicker main inflorescences of *Pro35S::AfSPL14* transgenic plants under LD conditions. (f) The diameter of main inflorescences of WT, Vector and transgenic plants. Forty-eight 38-day-old, long-day-grown plants were counted for each line. The diameter of the positions which were 5 cm distance from the basal of the main inflorescences was measured. ANOVA was conducted, and means were separated by DNMRT.

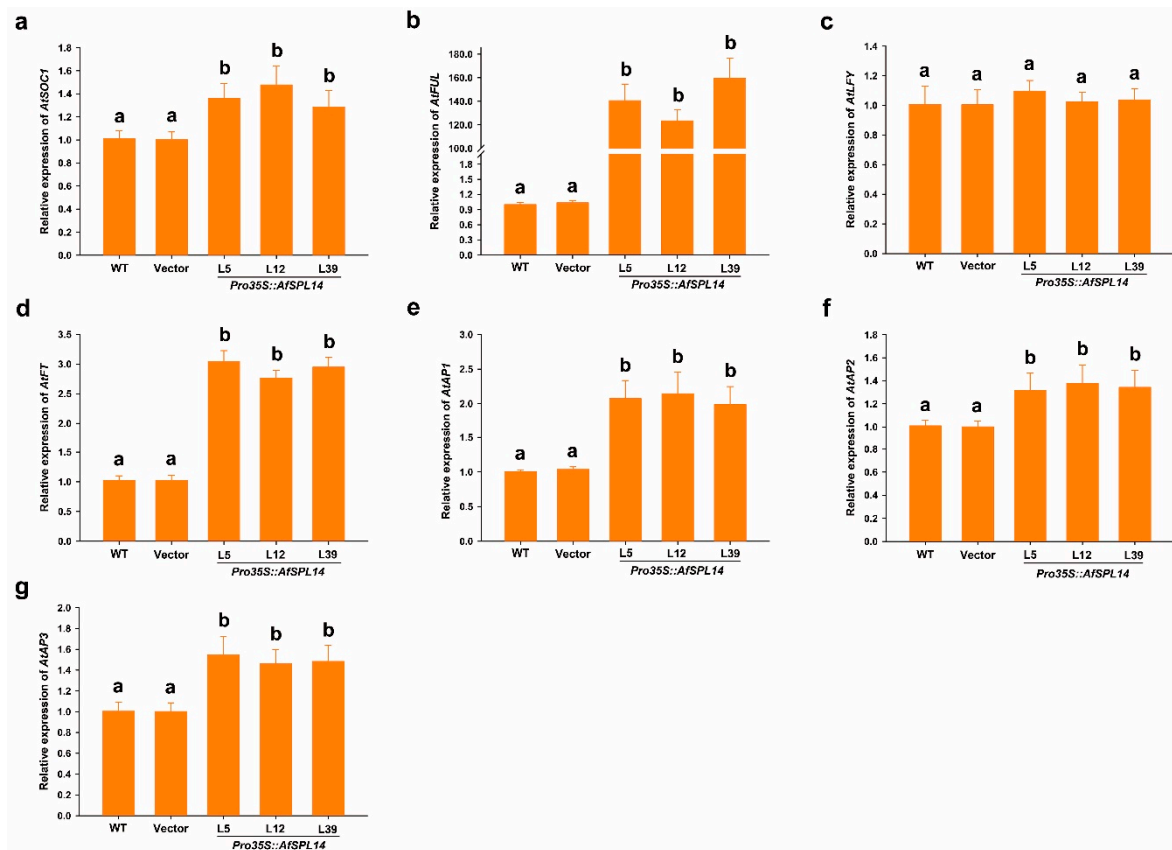


Figure 7. RT-qPCR analysis of flowering related genes at the shoot apex of WT, Vector and *Pro35S::AfSPL14* transgenic plants. Relative expression of three flowering promoting genes, *SUPPRESSOR OF OVEREXPRESSION OF CONSTANS 1 (SOC1)* (a), *FRUITFULL (FUL)* (b), *LEAFY* (c), and one florigen *Flowering Locus T (FT)* (d), and three flowering organ identify genes, *APETALA1 (AP1)* (e), *AP2* (f) and *AP3* (g) was performed. Fourteen-day-old long-day-grown seedlings were used. Three biological replicates and three technical replicates were performed. Transcript levels were normalized using *AtACTB* gene as a reference. All primers used here are listed in Table S3 online. ANOVA was conducted, and means were separated by DNMRT.

3. Discussion

SPL proteins are plant-specific TFs, and have been reported in many plants, including *Antirrhinum majus* [2], *Arabidopsis thaliana* [3], *Chlamydomonas* [14], *O. sativa* [36], *P. patens* [5], tomato [38], *Triticum aestivum* [39], *Castor Bean* [40], *Prunus mume* [41], *Citrus* [42], pepper [43], *Petunia* [44], *Brassica napus* [45] and *Chrysanthemum* [46]. In the present study, we identified the SPL gene *AfSPL14* in *A. fasciata*, an economically valuable, short-day ornamental plant that exhibits crassulacean acid metabolism (CAM). We discussed the correlation between this gene and the plant hormone ethylene, which has been widely used to induce flowering of members in numbers of the Bromeliaceae family. We also suggested that *AfSPL14* was a putative flowering inducer and ideal plant architecture generator, based on its heterologous constitutive expression in *Arabidopsis*.

Compared with many other plant species in which the role of ethylene in the regulation of flowering appears complicated, in a majority of bromeliads including pineapple and *A. fasciata*, flowering can be triggered by a small burst of ethylene production in the meristem in response to exogenous ethylene or ethephon treatment [30,33]. In previous studies, several ethylene biosynthesis, signaling and responsive genes were identified and characterized [30–33,47]. Here, we found that exogenous ethephon induced the expression of *AfSPL14* transcripts rapidly and dramatically within

1 h (Figure 4c). Interestingly, the expression level of *AfSPL14* transcripts gradually declined after continuous treatment for 8 h (Figure 4c). In fact, several *SPLs* in some other species also could be transiently upregulated and then downregulated by ethylene, for example, *MdSBP20* and *MdSBP27* in the leaves of apple (*Malus × domestica* Borkh.) cv. 'Fuji'34, and *SPL7* and *SPL9* in the fruit of *Cavendish banana* [48]. A more precise identification of the changes in the translational level of *AfSPL14* in response to the exogenous ethephon treatment showed a consistence with the changes at the transcriptional level. After treatment for 1 h, the expression of the *AfSPL14* protein was also dramatically induced to a higher level compared with that in the untreated central leaves (Figure 4d,e). However, after treatment for 8 h and 24 h, the amount of *AfSPL14* also decreased gradually (Figure 4d,e). Furthermore, three 5'-ATGTA-3' core sequences were enclosed in the nearly 3000-bp-length promoter sequence of *AfSPL14* promoter (Figure S2). The 5'-ATGTA-3' core sequence might interact with ethylene insensitive 3 (EIN3), a crucial factor in the ethylene signaling pathway that could activate or inhibit the expression of downstream genes at the transcriptional level. Further investigation should be performed regarding the regulation of *AfSPL14* by exogenous ethephon at the transcriptional and post-transcriptional levels.

Previous studies of the molecular regulation of the model species *Arabidopsis* have identified at least five genetic pathways relevant to flowering, namely: the photoperiod, vernalization, gibberellic acid (GA), and the autonomous and aging pathways [49]. During this process, at least 180 genes were involved [50]. *SPLs* are indispensable among these genes, and are involved in several signaling pathways. For example, *AtSPL3* and *AtSPL9* act independently of *FT*, and directly activate flower-promoting *MADS box* genes, thus defining a separate endogenous flowering pathway [18]. *AtSPL9* could also acts upstream of *FT* and promotes *FT* expression [51,52]. *AtSPL15* integrates the GA pathway and the aging pathway to promote flowering [53]. In addition, *AtSPL3/4/5* link developmental aging and photoperiodic flowering [54]. Moreover, the enhancement of the miR156 site-mutated *OsSPL14* gene could also accelerate flowering [55]. Phylogenetic and motif analyses of *AfSPL14* and the *SPLs* of *Arabidopsis* and *OsSPL14* showed that the former was similar to *AtSPL9*, *AtSPL15*, and *OsSPL14* (Figures 1–3), implying a putative conserved function, such as, flowering promotion. Recently, an age-dependent flowering pathway was identified by the regulation of *CmNF-YB8*, a nuclear factor, through directly triggering miR156-*SPL*-regulated processes in the short day plant chrysanthemum (*Chrysanthemum morifolium*) [56]. The flowering of pineapple and *A. fasciata* is also age dependent, and the juvenile plants cannot flower naturally, even when treated with exogenous ethylene [30,33]. The expression of *AfSPL14* transcripts was higher in the central leaves and stems of adult plants prior to flower bud differentiation compared with that of the juvenile plants (Figure 4a). This fact is similar to the increasing pattern of accumulation of *AtSPL9* and *AtSPL15* in the meristem with age [9,17,53], and inconsistent with the expression profile of *AfAP2-1*, a putative flowering TF encoding gene identified in *A. fasciata* [33]. These results suggest that *AfSPL14* might act positively in the juvenile-to-vegetative phase transition and flowering pathway regulated by developmental age.

The constitutive expression of *AfSPL14* in *Arabidopsis* significantly promoted flowering under LD conditions (Figure 6a–c), which was inconsistent with the flowering-delayed phenotype caused by the constitutive expression of *AfAP2-1* in *Arabidopsis* [33], thus suggesting that *AfSPL14* is an activator of flowering integrator and floral inductive genes such as *AtFT*, *AtAP1*, *AtSOC1*, and *AtFUL* (Figure 7a,b,d,e). A previous study demonstrated that the overexpression of *AtSPL3* could strongly induce *AtFUL*, but has a weaker effect, or no effect at all, on *AtSOC1* in the shoot apex in *Arabidopsis* [18]. Interestingly, compared with that of WT, the expression level of *AtFUL* at the shoot apex of *Pro35S::AfSPL14* transgenic plants was upregulated dramatically, while *AtSOC1* was slightly induced (Figure 7a,b), suggesting that similar to *AtSPL3*, *AfSPL14* might also induce flowering via an endogenous pathway.

Phylogenetic and motif analyses of *AfSPL14* with variable *SPLs* suggested that it was closer and more similar to *OsSPL14* than to *AtSPL9* and *AtSPL15* (Figures 2 and 3); this is consistent with

the evolutionary distances among *A. fasciata*, rice and *Arabidopsis*. In addition, the genes have similar exon-intron structures (Figure 3). Higher expression of *OsSPL14* could reduce the tiller number, increase the lodging resistance, promote panicle branching, and enhance the grain yield [25,26]. Importantly, in addition to the acceleration of flowering, the constitutive expression of *AfSPL14* in *Arabidopsis* also promotes the number of main inflorescences and produces thicker and sturdier culms (Figure 6a–f). However, we did not find the transactivator activity of *AfSPL14* in yeast cells (Figure 5), in opposition to the results reported on *OsSPL14* [26]. These results suggested functional conservation and diversification in *AfSPL14* and *OsSPL14*. Interestingly, the repression of *AtSPL10* caused reduced apical dominance, and increased the number of main inflorescences [10]. A loss-of-function mutation of *AtSPL9* and *AtSPL15* resulted in altered main stem architecture and enhanced branching [17]. The main inflorescence-changed phenotypes of constitutive expressed *AfSPL14* in *Arabidopsis* and loss-of-function *AtSPL9*, *AtSPL10*, and *AtSPL15* mutants appeared to be similar.

Certain SPLs can be regulated by miR156, two miRNAs that can regulate the expression of SPL proteins at the post-transcriptional level [57]. Similar to *OsSPL14*, *AfSPL14* also had a miR156 cleavage site in its CDS sequence (Figure 3). Because of a point mutation in the OsmiR156-directed site of *OsSPL14*, grain yield was enhanced [25,26]. Many SPLs positively regulate grain yield [23,58–60]. The thicker main inflorescence phenotype in *AfSPL14*-constitutive expressed *Arabidopsis* implied that this gene might act positively in the regulation of flower stalk diameter in *A. fasciata*. Further investigation should focus on the morphological changes of flowers in *AfSPL14*-overexpressed and/or *AfSPL14*-silenced *A. fasciata*, the morphological changes of flowers in *AfSPL14*-overexpressed and/or *AfSPL14*-silenced pineapple, and the cloning and functional characterization of possible homologs of *AfSPL14* in pineapple.

4. Materials and Methods

4.1. Plant Materials and Sample Preparation

The *A. fasciata* specimens used in this study were planted in a greenhouse (ambient temperature of 30–32 °C) located in the experimental area of the Institute of Tropical Crop Genetic Resources, Chinese Academy of Tropical Agricultural Sciences (CATAS). For the tissue-specific expression and western blot analyses, different tissue samples, including mature leaves, central leaves, stems, roots, and various flower organs, were collected.

The wild-type (WT) and transgenic plants of *Arabidopsis* used in this study were of the Columbia ecotype (Col-0). Seeds were surface sterilized in 0.1% HgCl₂ for 10 min and then washed with sterilized distilled water five times. The washed seeds were then plated on MS medium containing sugar (2%) and agar (0.8%) and incubated in the dark at 4 °C for 2 days. The plates were then moved to a chamber at 23 °C under LD (16 h light) conditions, with a photon flux density (120 μmol m⁻² s⁻¹) for continuous growth.

4.2. Isolation and Sequencing of the *AfSPL14* Gene

Total RNA was extracted from the central leaves of *A. fasciata* using the hexadecyl trimethyl ammonium bromide (CTAB) method [33], and then used for the RACE at the 5' and 3' ends according to the manufacturer's instructions for the SMARTer™ RACE cDNA Amplification Kit (Clontech, Tokyo, Japan). The specific 5' and 3' fragments were cloned into pEASY-blunt vectors (Transgen, Beijing, China), and then sequenced by Thermo Fisher Scientific (Guangzhou, China). The gene accession number of *AfSPL14* is MF114304. The primers used here are listed in Table S3 online.

4.3. Bioinformatic Analysis

The ORF of *AfSPL14* was predicted using the ORF Finder (<https://www.ncbi.nlm.nih.gov/orffinder/>). The sequence logo was generated by the online WebLogo 3 platform (<http://weblogo.threeplusone.com/>). A phylogenetic tree was constructed with MEGA version 6.0 using

the neighbor-joining method with 1000 bootstrap replications [61]. The scheme of exon-intron structures was generated by Gene Structure Display Server 2.0 (<http://gsds.cbi.pku.edu.cn/index.php>). Putative motifs of variable SPLs were identified by MEME software online with default settings (<http://meme-suite.org/tools/meme>).

4.4. 5' RLM-RACE

5' RLM-RACE was performed according to the manufacturer's instructions of FirstChoice[®] RLM-RACE Kit (Thermo Fisher Scientific, New York, NY, USA). For the next amplification, 10 µg of total RNA, which was isolated from central leaves of 12-month-old *A. fasciata* plants using the CTAB method [33], was used. The gene specific primers of *AfSPL14* for the first and second PCR products are *AfSPL14*-5outer and *AfSPL14*-5inner, respectively. The second PCR products were gel purified and subcloned into pEASY-T3 Vector (Transgen, Beijing, China) for sequencing. Primers used for 5' modified RACE are listed in Table S3 online.

4.5. RT-qPCR

First-strand cDNA was synthesized using the TransScript One-Step gDNA Removal and cDNA Synthesis SuperMix (Transgen, Beijing, China) according to the manufacturer's instructions. Quantitative real-time PCR (qPCR) was conducted on a Thermo PikoReal 96[™] Real-Time PCR System (Thermo Fisher Scientific, Waltham, MA, USA) using the TransStart Tip Green qPCR SuperMix Kit (Transgen, Beijing, China). The total reactions (20 µL) described in this protocol converted total RNA (500 ng ~ 5 µg) into the first-strand cDNA. The first-strand reaction products (20 µL) were diluted with sterilized distilled H₂O 5 times, and diluted products (1 µL) were used for total qPCR reactions (10 µL). Three biological replicates and three technical replicates were performed. The relative expression levels of specific genes were calculated using the $2^{-\Delta\Delta C_t}$ method with the β -actin gene (*ACTB*) of *A. fasciata* or *Arabidopsis* as the internal control [62]. All primers used for qPCR are listed in Table S3 online.

4.6. Transgenic Plants

For the transgenic constructs, the coding sequence (CDS) of *AfSPL14* was cloned into the KpnI-SalI sites of the binary vector Cam35S-gfp under the control of the cauliflower mosaic virus (CaMV) 35S promoter. The constructs were then delivered into *Agrobacterium tumefaciens* strain EHA105 by the freeze-thaw method [63]. Col-0 background *Arabidopsis* was transformed using the floral dipping method [64]. For the selection of transgenic plants, the seeds were planted on MS agar medium supplemented with hygromycin (25 mg/L). Seedlings conferring resistance to hygromycin were then transplanted in a chamber at 23 °C under LD conditions. Transgenic plants were verified by genomic PCR and RT-PCR using primers *AfSPL14*-OX F and *AfSPL14*-OX R, which were listed in Table S3 online. T3 transgenic plants were used for next experiments.

4.7. Transactivation Analysis of *AfSPL14* in Yeast Cells

The yeast strain Y2HGold was transformed with plasmids containing the pGBKT7 (pBD) vector with the ORF or fragments of *AfSPL14* fused in frame with GAL4 DNA binding domain. The primers used are listed in Table S3 online. pBD and pGAL4 were used as negative and positive controls, respectively. Transformants were selected on synthetic dropout (SD) medium lacking tryptophan (SD/–Trp) (Clontech, Tokyo, Japan) and then dripped onto SD/–Trp/+AbA/+X-α-gal to determine the transactivation activity.

4.8. Exogenous Ethephon Treatment of *A. fasciata*

To test the response to ethylene, adult (12-month-old) *A. fasciata* plants which were grown in pots in our greenhouse were treated with ethephon (10 mL) at 0.3 g·L⁻¹, 0.6 g·L⁻¹, 1.2 g·L⁻¹, 2.4 g·L⁻¹, 4.8 g·L⁻¹ for 1, 2, 4, 8, 24, or 48 h. All treatments were applied by pouring the specific

concentration of ethephon solution into the leaf whorl of each plant, with the same quantity of water as control. The central leaves were then physically isolated and immediately frozen in liquid nitrogen for further research.

4.9. SDS-PAGE and Immunoblot Analysis

Total proteins were extracted from the central leaves of adult *A. fasciata* plants. The physically isolated and immediately frozen central leaves (0.5 g) were homogenized with extraction buffer (1 mL) (Tris (1 mol/L, pH 6.8); DL-dithiothreitol (0.2 mol/L); sodium dodecyl sulfate (4% (g/mL)); glycerol (20%)) by using pestle and mortar. After centrifugation at 12,000 rotation per minute (rpm) for 15 min at 4 °C, the supernatants were transferred into new tubes and 4 times volume of acetones were added. After being vortexed for 2 min and then placed on ice for 1 h, the mixture was centrifuged again, as above. The supernatants were discarded and 4 times volume of acetone was added. The mixture was then vortexed and centrifuged again; the extracted proteins were diluted with 0.5× extraction buffer, boiled at 100 °C for 10 min, and then centrifuged at 13,000 rpm for 5 min. The supernatants (total central leaf proteins) were separated using 15% sodium dodecyl sulfate polyacrylamide gel electrophoresis (SDS-PAGE) containing urea (6 mol/L). After electrophoresis, the proteins were transferred onto nitrocellulose membranes (Amersham Biosciences, Pittsburgh, PA, USA) and probed with a rabbit polyclonal AfSPL14 antibody (Jiaxuan Biotech, Beijing, China) or a rabbit polyclonal Actin antibody (Agrisera, Vännäs, Sweden). After incubation with horseradish peroxidase conjugated goat anti-rabbit IgG (Jiaxuan Biotech, Beijing, China), the signals were detected by enhanced chemiluminescence (Jiaxuan Biotech, Beijing, China). X-ray films were scanned and analyzed using ImageMaster™ 2D Platinum software (GE Healthcare, Pittsburgh, PA, USA). Protein concentration of each extract was determined by using a protein assay kit (Bio-Rad, Hercules, CA, USA) with BSA as the standard.

4.10. Data Analysis

Values represent means ± standard deviation of two or three biological replicates. ANOVA was conducted, and the means were separated by Duncan's New Multiple Range Test (DNMRT).

Supplementary Materials: Supplementary materials can be found at <http://www.mdpi.com/1422-0067/19/7/2085/s1>.

Author Contributions: Conceptualization, L.X. and M.L.; Methodology, L.X.; Software, J.-b.W.; Validation, M.L., and L.X.; Formal Analysis, J.-b.W.; Investigation, M.L. and M.-f.A.; Resources, Z.-y.L., Y.-l.F. and L.X.; Data Curation, M.L., J.-b.W. and M.-f.A.; Writing-Original Draft Preparation, M.L.; Writing-Review & Editing, L.X.

Acknowledgments: This work was supported by grants from the National Natural Science Foundation of China (31372106, 31601793), the National Science Foundation of Hainan Province (20163127) and the Fundamental Scientific Research Funds for CATAS-TCGRI (1630032016006).

Conflicts of Interest: The authors declare no conflict of interest.

Abbreviations

SBP	SQUAMOSA PROMOTER BINDING PROTEIN
SPL	SBP-LIKE
miRNA	microRNA
TGA1	TEOSINTE GLUME ARCHITECTURE
LD	long day
RACE	Rapid amplification of cDNA ends
UTR	Untranslated region
ORF	Open reading frame
MW	Molecular weight
pI	Isoelectric point
Jp	Joint peptide
NLS	Nuclear localization signal

RT-qPCR	Reverse transcription followed by quantitative real-time PCR
RLM-RACE	RNA ligase mediated rapid amplification of cDNA ends
DAF	Day after flowering
WT	Wild Type
SOC1	SUPPRESSOR OF OVEREXPRESSION OF CONSTANS 1
FUL	FRUITFULL
AP1	APETALA1
LFY	LEAFY
FT	Flowering Locus T
AP2	APETALA2
AP3	APETALA3
CAM	Crassulacean acid metabolism
EIN3	ETHYLENE INSENSITIVE 3
GA	Gibberellic acid
CTAB	Hexadecyl trimethyl ammonium bromide
CDS	the coding sequence
SDS-PAGE	Sodium dodecyl sulfate polyacrylamide gel electrophoresis

References

1. Preston, J.C.; Hileman, L.C. Functional evolution in the plant *SQUAMOSA-PROMOTER BINDING PROTEIN-LIKE* (SPL) gene family. *Front. Plant Sci.* **2013**, *4*, 80. [[CrossRef](#)] [[PubMed](#)]
2. Klein, J.; Saedler, H.; Huijser, P. A new family of DNA binding proteins includes putative transcriptional regulators of the *Antirrhinum majus* floral meristem identity gene *SQUAMOSA*. *Mol. Gen. Genet.* **1996**, *250*, 7–16. [[PubMed](#)]
3. Cardon, G.H.; Hohmann, S.; Nettessheim, K.; Saedler, H.; Huijser, P. Functional analysis of the *Arabidopsis thaliana* *SBP-box* gene *SPL3*: A novel gene involved in the floral transition. *Plant J.* **1997**, *12*, 367–377. [[CrossRef](#)] [[PubMed](#)]
4. Arazi, T.; Talmor-Neiman, M.; Stav, R.; Riese, M.; Huijser, P.; Baulcombe, D.C. Cloning and characterization of micro-RNAs from moss. *Plant J.* **2005**, *43*, 837–848. [[CrossRef](#)] [[PubMed](#)]
5. Riese, M.; Höhmann, S.; Saedler, H.; Münster, T.; Huijser, P. Comparative analysis of the *SBP-box* gene families in *P. patens* and seed plants. *Gene* **2007**, *401*, 28–37. [[CrossRef](#)] [[PubMed](#)]
6. Yamasaki, K.; Kigawa, T.; Inoue, M.; Tateno, M.; Yamasaki, T.; Yabuki, T.; Aoki, M.; Seki, E.; Matsuda, T.; Nunokawa, E.; Ishizuka, Y.; et al. A novel zinc-binding motif revealed by solution structures of DNA-binding domains of *Arabidopsis* SBP-family transcription factors. *J. Mol. Biol.* **2004**, *337*, 49–63. [[CrossRef](#)] [[PubMed](#)]
7. Moreno, M.A.; Harper, L.C.; Krueger, R.W.; Dellaporta, S.L.; Freeling, M. *Liguleless1* encodes a nuclear-localized protein required for induction of ligules and auricles during maize leaf organogenesis. *Genes Dev.* **1997**, *11*, 616–628. [[CrossRef](#)] [[PubMed](#)]
8. Lee, J.; Park, J.J.; Kim, S.L.; Yim, J.; An, G. Mutations in the rice *liguleless* gene result in a complete loss of the auricle, ligule, and laminar joint. *Plant Mol. Biol.* **2007**, *65*, 487–499. [[CrossRef](#)] [[PubMed](#)]
9. Wang, J.W.; Schwab, R.; Czech, B.; Mica, E.; Weigel, D. Dual effects of miR156-targeted *SPL* genes and *CYP78A5/KLUH* on plastochron length and organ size in *Arabidopsis thaliana*. *Plant Cell* **2008**, *20*, 1231–1243. [[CrossRef](#)] [[PubMed](#)]
10. Shikata, M.; Koyama, T.; Mitsuda, N.; Ohme-Takagi, M. *Arabidopsis* *SBP-box* genes *SPL10*, *SPL11* and *SPL2* control morphological change in association with shoot maturation in the reproductive phase. *Plant Cell Physiol.* **2009**, *50*, 2133–2145. [[CrossRef](#)] [[PubMed](#)]
11. Nodine, M.D.; Bartel, D.P. MicroRNAs prevent precocious gene expression and enable pattern formation during plant embryogenesis. *Genes Dev.* **2010**, *24*, 2678–2692. [[CrossRef](#)] [[PubMed](#)]
12. Xing, S.; Salinas, M.; Hohmann, S.; Berndtgen, R.; Huijser, P. miR156-targeted and nontargeted SBP-box transcription factors act in concert to secure male fertility in *Arabidopsis*. *Plant Cell* **2010**, *22*, 3935–3950. [[CrossRef](#)] [[PubMed](#)]

13. Xing, S.; Salinas, M.; Garcia-Molina, A.; Hohmann, S.; Berndtgen, R.; Huijser, P. *SPL8* and miR156-targeted *SPL* genes redundantly regulate *Arabidopsis* gynoecium differential patterning. *Plant J.* **2013**, *75*, 566–577. [[CrossRef](#)] [[PubMed](#)]
14. Kropat, J.; Tottey, S.; Birkenbihl, R.P.; Depege, N.; Huijser, P.; Merchant, S. A regulator of nutritional copper signaling in *Chlamydomonas* is an SBP domain protein that recognizes the GTAC core of copper response element. *Proc. Natl. Acad. Sci. USA* **2005**, *102*, 18730–18735. [[CrossRef](#)] [[PubMed](#)]
15. Yamasaki, H.; Hayashi, M.; Fukazawa, M.; Kobayashi, Y.; Shikanai, T. SQUAMOSA promoter binding protein-like7 is a central regulator for copper homeostasis in *Arabidopsis*. *Plant Cell* **2009**, *21*, 347–361. [[CrossRef](#)] [[PubMed](#)]
16. Wu, G.; Poethig, R.S. Temporal regulation of shoot development in *Arabidopsis thaliana* by miR156 and its target *SPL3*. *Development* **2006**, *133*, 3539–3547. [[CrossRef](#)] [[PubMed](#)]
17. Schwarz, S.; Grande, A.V.; Bujdoso, N.; Saedler, H.; Huijser, P. The microRNA regulated *SBP-box* genes *SPL9* and *SPL15* control shoot maturation in *Arabidopsis*. *Plant Mol. Biol.* **2008**, *67*, 183–195. [[CrossRef](#)] [[PubMed](#)]
18. Wang, J.W.; Czech, B.; Weigel, D. MiR156-regulated *SPL* transcription factors define an endogenous flowering pathway in *Arabidopsis thaliana*. *Cell* **2009**, *138*, 738–749. [[CrossRef](#)] [[PubMed](#)]
19. Yamaguchi, A.; Wu, M.F.; Yang, L.; Wu, G.; Poethig, R.S.; Wagner, D. The microRNA-regulated *SBP-box* transcription factor *SPL3* is a direct upstream activator of *LEAFY*, *FRUITFULL*, and *APETALA1*. *Dev. Cell* **2009**, *17*, 268–278. [[CrossRef](#)] [[PubMed](#)]
20. Stone, J.M.; Liang, X.; Nekl, E.R.; Stiers, J.J. *Arabidopsis* AtSPL14, a plant-specific SBP-domain transcription factor, participates in plant development and sensitivity to fumonisin B1. *Plant J.* **2005**, *41*, 744–754. [[CrossRef](#)] [[PubMed](#)]
21. Wang, H.; Nussbaum-Wagler, T.; Li, B.; Zhao, Q.; Vigouroux, Y.; Faller, M.; Bomblies, K.; Lukens, L.; Doebley, J.F. The origin of the naked grains of maize. *Nature* **2005**, *436*, 714–719. [[CrossRef](#)] [[PubMed](#)]
22. Liu, J.; Cheng, X.; Liu, P.; Sun, J. miR156-regulated TaSPLs interact with TaD53 to regulate *TaTB1* and *TaBA1* expression in bread wheat. *Plant Physiol.* **2017**, *174*, 1931–1948. [[CrossRef](#)] [[PubMed](#)]
23. Zhang, B.; Xu, W.; Liu, X.; Mao, X.; Li, A.; Wang, J.; Chang, X.; Zhang, X.; Jing, R. Functional conservation and divergence among homoeologs of *TaSPL20* and *TaSPL21*, two *SBP-box* genes governing yield-related traits in hexaploid wheat. *Plant Physiol.* **2017**, *174*, 1177–1191. [[CrossRef](#)] [[PubMed](#)]
24. Gou, J.; Fu, C.; Liu, S.; Tang, C.; Debnath, S.; Flanagan, A.; Ge, Y.; Tang, Y.; Jiang, Q.; Larson, P.R.; Wen, J.; Wang, Z.Y. The miR156-SPL4 module predominantly regulates aerial axillary bud formation and controls shoot architecture. *New Phytol.* **2017**, *216*, 829–840. [[CrossRef](#)] [[PubMed](#)]
25. Jiao, Y.; Wang, Y.; Xue, D.; Wang, J.; Yan, M.; Liu, G.; Dong, G.; Zeng, D.; Lu, Z.; Zhu, X.; et al. Regulation of *OsSPL14* by *OsmiR156* defines ideal plant architecture in rice. *Nat. Genet.* **2010**, *42*, 541–544. [[CrossRef](#)] [[PubMed](#)]
26. Miura, K.; Ikeda, M.; Matsubara, A.; Song, X.J.; Ito, M.; Asano, K.; Matsuoka, M.; Kitano, H.; Ashikari, M. *OsSPL14* promotes panicle branching and higher grain productivity in rice. *Nat. Genet.* **2010**, *42*, 545–549. [[CrossRef](#)] [[PubMed](#)]
27. Givnish, T.J.; Barfuss, M.H.; Van Ee, B.; Riina, R.; Schulte, K.; Horres, R.; Gonsiska, P.A.; Jabaily, R.S.; Crayn, D.M.; Smith, J.A.; et al. Phylogeny, adaptive radiation, and historical biogeography in Bromeliaceae: Insights from an eight-locus plastid phylogeny. *Am. J. Bot.* **2011**, *98*, 872–895. [[CrossRef](#)] [[PubMed](#)]
28. Zanella, C.M.; Janke, A.; Palma-Silva, C.; Kaltchuk-Santos, E.; Pinheiro, F.G.; Paggi, G.M.; Soares, L.E.; Goetze, M.; Buttow, M.V.; Bered, F. Genetics, evolution and conservation of Bromeliaceae. *Genet. Mol. Biol.* **2012**, *35*, 1020–1026. [[CrossRef](#)] [[PubMed](#)]
29. Bartholomew, D.P.; Paull, R.E.; Rohrbach, K.G. *The Pineapple-Botany, Production and Uses*; CABI Publishing: Wallingford, UK, 2003; p. 176.
30. Trusov, Y.; Botella, J.R. Silencing of the *ACC synthase* gene *ACACS2* causes delayed flowering in pineapple [*Ananas comosus* (L.) Merr.]. *J. Exp. Bot.* **2006**, *57*, 3953–3960. [[CrossRef](#)] [[PubMed](#)]
31. Lv, L.; Duan, J.; Xie, J.; Wei, C.; Liu, Y.; Liu, S.; Sun, G. Isolation and characterization of a *FLOWERING LOCUS T* homolog from pineapple (*Ananas comosus* (L.) Merr). *Gene* **2012**, *505*, 368–373. [[CrossRef](#)] [[PubMed](#)]
32. Lv, L.L.; Duan, J.; Xie, J.H.; Liu, Y.G.; Wei, C.B.; Liu, S.H.; Zhang, J.X.; Sun, G.M. Cloning and expression analysis of a *PISTILLATA* homologous gene from pineapple (*Ananas comosus* L. Merr). *Int. J. Mol. Sci.* **2012**, *13*, 1039–1053. [[CrossRef](#)] [[PubMed](#)]

33. Lei, M.; Li, Z.Y.; Wang, J.B.; Fu, Y.L.; Ao, M.F.; Xu, L. *AfAP2-1*, An age-dependent gene of *Aechmea fasciata*, responds to exogenous ethylene treatment. *Int. J. Mol. Sci.* **2016**, *17*, 303. [[CrossRef](#)] [[PubMed](#)]
34. Li, J.; Hou, H.; Li, X.; Xiang, J.; Yin, X.; Gao, H.; Zheng, Y.; Bassett, C.L.; Wang, X. Genome-wide identification and analysis of the *SBP-box* family genes in apple (*Malus x domestica* Borkh.). *Plant Physiol. Biochem.* **2013**, *70*, 100–114. [[CrossRef](#)] [[PubMed](#)]
35. Bailey, T.L.; Elkan, C. Fitting a mixture model by expectation maximization to discover motifs in biopolymers. *Int. Conf. Intell. Syst. Mol. Biol.* **1994**, *2*, 28–36.
36. Xie, K.; Wu, C.; Xiong, L. Genomic organization, differential expression, and interaction of *SQUAMOSA* promoter-binding-like transcription factors and microRNA156 in rice. *Plant Physiol.* **2006**, *142*, 280–293. [[CrossRef](#)] [[PubMed](#)]
37. Li, Z.; Wang, J.; Zhang, X.; Lei, M.; Fu, Y.; Zhang, J.; Wang, Z.; Xu, L. Transcriptome sequencing determined flowering pathway genes in *Aechmea fasciata* treated with ethylene. *J. Plant Growth Regul.* **2016**, *35*, 316–329. [[CrossRef](#)]
38. Salinas, M.; Xing, S.; Hohmann, S.; Berndtgen, R.; Huijser, P. Genomic organization, phylogenetic comparison and differential expression of the *SBP-box* family of transcription factors in tomato. *Planta* **2012**, *235*, 1171–1184. [[CrossRef](#)] [[PubMed](#)]
39. Zhang, B.; Liu, X.; Zhao, G.; Mao, X.; Li, A.; Jing, R. Molecular characterization and expression analysis of *Triticum aestivum squamosa-promoter binding protein-box* genes involved in ear development. *J. Integr. Plant Biol.* **2013**, *56*, 571–581. [[CrossRef](#)] [[PubMed](#)]
40. Zhang, S.; Ling, L. Genome-wide identification and evolutionary analysis of the *SBP-box* gene family in castor bean. *PLoS ONE* **2014**, *9*, e86688. [[CrossRef](#)] [[PubMed](#)]
41. Xu, Z.; Sun, L.; Zhou, Y.; Yang, W.; Cheng, T.; Wang, J.; Zhang, Q. Identification and expression analysis of the *SQUAMOSA promoter-binding protein (SBP)-box* gene family in *Prunus mume*. *Mol. Genet. Genom.* **2015**, *290*, 1701–1715. [[CrossRef](#)] [[PubMed](#)]
42. Shalom, L.; Shlizerman, L.; Zur, N.; Doron-Faigenboim, A.; Blumwald, E.; Sadka, A. Molecular characterization of *SQUAMOSA PROMOTER BINDING PROTEIN-LIKE (SPL)* gene family from *Citrus* and the effect of fruit load on their expression. *Front. Plant Sci.* **2015**, *6*, 389. [[CrossRef](#)] [[PubMed](#)]
43. Zhang, H.X.; Jin, J.H.; He, Y.M.; Lu, B.Y.; Li, D.W.; Chai, W.G.; Khan, A.; Gong, Z.H. Genome-wide identification and analysis of the *SBP-box* family genes under *Phytophthora capsici* stress in pepper (*Capsicum annuum* L.). *Front. Plant Sci.* **2016**, *7*, 504. [[CrossRef](#)] [[PubMed](#)]
44. Preston, J.C.; Jorgensen, S.A.; Orozco, R.; Hileman, L.C. Paralogous *SQUAMOSA PROMOTER BINDING PROTEIN-LIKE (SPL)* genes differentially regulate leaf initiation and reproductive phase change in petunia. *Planta* **2016**, *243*, 429–440. [[CrossRef](#)] [[PubMed](#)]
45. Cheng, H.; Hao, M.; Wang, W.; Mei, D.; Tong, C.; Wang, H.; Liu, J.; Fu, L.; Hu, Q. Genomic identification, characterization and differential expression analysis of *SBP-box* gene family in *Brassica napus*. *BMC Plant Biol.* **2016**, *16*, 196. [[CrossRef](#)] [[PubMed](#)]
46. Song, A.; Gao, T.; Wu, D.; Xin, J.; Chen, S.; Guan, Z.; Wang, H.; Jin, L.; Chen, F. Transcriptome-wide identification and expression analysis of *chrysanthemum* *SBP*-like transcription factors. *Plant Physiol. Biochem.* **2016**, *102*, 10–16. [[CrossRef](#)] [[PubMed](#)]
47. Li, Y.H.; Wu, Q.S.; Huang, X.; Liu, S.H.; Zhang, H.N.; Zhang, Z.; Sun, G.M. Molecular cloning and characterization of four genes encoding ethylene receptors associated with pineapple (*Ananas comosus* L.) flowering. *Front. Plant Sci.* **2016**, *7*, 710. [[CrossRef](#)] [[PubMed](#)]
48. Bi, F.; Meng, X.; Ma, C.; Yi, G. Identification of miRNAs involved in fruit ripening in Cavendish bananas by deep sequencing. *BMC Genom.* **2015**, *16*, 776. [[CrossRef](#)] [[PubMed](#)]
49. Srikanth, A.; Schmid, M. Regulation of flowering time: All roads lead to Rome. *Cell. Mol. Life Sci.* **2011**, *68*, 2013–2037. [[CrossRef](#)] [[PubMed](#)]
50. Fornara, F.; de Montaigu, A.; Coupland, G. SnapShot: Control of flowering in *Arabidopsis*. *Cell* **2010**, *141*, 550. [[CrossRef](#)] [[PubMed](#)]
51. Jung, J.H.; Seo, Y.H.; Seo, P.J.; Reyes, J.L.; Yun, J.; Chua, N.H.; Park, C.M. The *GIGANTEA*-regulated microRNA172 mediates photoperiodic flowering independent of *CONSTANS* in *Arabidopsis*. *Plant Cell* **2007**, *19*, 2736–2748. [[CrossRef](#)] [[PubMed](#)]
52. Wu, G.; Park, M.Y.; Conway, S.R.; Wang, J.W.; Weigel, D.; Poethig, R.S. The sequential action of miR156 and miR172 regulates developmental timing in *Arabidopsis*. *Cell* **2009**, *138*, 750–759. [[CrossRef](#)] [[PubMed](#)]

53. Hyun, Y.; Richter, R.; Vincent, C.; Martinez-Gallegos, R.; Porri, A.; Coupland, G. Multi-layered regulation of *SPL15* and cooperation with *SOC1* integrate endogenous flowering pathways at the *Arabidopsis* shoot meristem. *Dev. Cell* **2016**, *37*, 254–266. [[CrossRef](#)] [[PubMed](#)]
54. Jung, J.H.; Lee, H.J.; Ryu, J.Y.; Park, C.M. *SPL3/4/5* integrate developmental aging and photoperiodic signals into the FT-FD module in *Arabidopsis* flowering. *Mol. Plant* **2016**, *9*, 1647–1659. [[CrossRef](#)] [[PubMed](#)]
55. Luo, L.; Li, W.; Miura, K.; Ashikari, M.; Kyoizuka, J. Control of tiller growth of rice by *OsSPL14* and Strigolactones, which work in two independent pathways. *Plant Cell Physiol.* **2012**, *53*, 1793–1801. [[CrossRef](#)] [[PubMed](#)]
56. Wei, Q.; Ma, C.; Xu, Y.; Wang, T.; Chen, Y.; Lu, J.; Zhang, L.; Jiang, C.Z.; Hong, B.; Gao, J. Control of *chrysanthemum* flowering through integration with an aging pathway. *Nat. Commun.* **2017**, *8*, 829. [[CrossRef](#)] [[PubMed](#)]
57. Ling, L.Z.; Zhang, S.D. Exploring the evolutionary differences of *SBP-box* genes targeted by miR156 and miR529 in plants. *Genetica* **2012**, *140*, 317–324. [[CrossRef](#)] [[PubMed](#)]
58. Wang, S.; Wu, K.; Yuan, Q.; Liu, X.; Liu, Z.; Lin, X.; Zeng, R.; Zhu, H.; Dong, G.; Qian, Q.; et al. Control of grain size, shape and quality by *OsSPL16* in rice. *Nat. Genet.* **2012**, *44*, 950–954. [[CrossRef](#)] [[PubMed](#)]
59. Chuck, G.S.; Brown, P.J.; Meeley, R.; Hake, S. Maize *SBP-box* transcription factors *unbranched2* and *unbranched3* affect yield traits by regulating the rate of lateral primordia initiation. *Proc. Natl. Acad. Sci. USA* **2014**, *111*, 18775–18780. [[CrossRef](#)] [[PubMed](#)]
60. Si, L.; Chen, J.; Huang, X.; Gong, H.; Luo, J.; Hou, Q.; Zhou, T.; Lu, T.; Zhu, J.; Shangguan, Y.; et al. *OsSPL13* controls grain size in cultivated rice. *Nat. Genet.* **2016**, *48*, 447–456. [[CrossRef](#)] [[PubMed](#)]
61. Tamura, K.; Stecher, G.; Peterson, D.; FilipSKI, A.; Kumar, S. MEGA6: Molecular Evolutionary Genetics Analysis version 6.0. *Mol. Biol. Evol.* **2013**, *30*, 2725–2729. [[CrossRef](#)] [[PubMed](#)]
62. Livak, K.J.; Schmittgen, T.D. Analysis of relative gene expression data using real-time quantitative PCR and the $2^{-\Delta\Delta CT}$ method. *Methods* **2001**, *25*, 402–408. [[CrossRef](#)] [[PubMed](#)]
63. Holsters, M.; de Waele, D.; Depicker, A.; Messens, E.; van Montagu, M.; Schell, J. Transfection and transformation of *Agrobacterium tumefaciens*. *Mol. Genet. Genom.* **1978**, *163*, 181–187. [[CrossRef](#)]
64. Clough, S.J.; Bent, A.F. Floral dip: A simplified method for *Agrobacterium*-mediated transformation of *Arabidopsis thaliana*. *Plant J.* **1998**, *16*, 735–743. [[CrossRef](#)] [[PubMed](#)]



© 2018 by the authors. Licensee MDPI, Basel, Switzerland. This article is an open access article distributed under the terms and conditions of the Creative Commons Attribution (CC BY) license (<http://creativecommons.org/licenses/by/4.0/>).